World Journal of Orthopedics

Submit a Manuscript: https://www.f6publishing.com

*World J Orthop* 2025 December 18; 16(12): 113320

DOI: 10.5312/wjo.v16.i12.113320

ISSN 2218-5836 (online)

ORIGINAL ARTICLE

Basic Study

# Altered lineage commitment of bone marrow mesenchymal stem cells in idiopathic osteonecrosis of the femoral head

Adrián Cardín-Pereda, Daniel García-Sánchez, Itziar Álvarez-Iglesias, Jennifer Cabello-Sanz, Flor M Pérez-Campo

**Specialty type:** Orthopedics

**Provenance and peer review:** Unsolicited article; Externally peer reviewed.

**Peer-review model:** Single blind

**Peer-review report's classification**

**Scientific Quality:** Grade B, Grade C, Grade C, Grade C

**Novelty:** Grade A, Grade B, Grade C, Grade C

**Creativity or Innovation:** Grade A, Grade C, Grade C, Grade C

**Scientific Significance:** Grade B, Grade B, Grade C, Grade C

**P-Reviewer:** Liu W, PhD, Associate Chief Physician, China; Lu Y, Associate Chief Physician, China; Zhang W, MD, China

**Received:** August 22, 2025

**Revised:** September 18, 2025

**Accepted:** November 6, 2025

**Published online:** December 18, 2025

**Processing time:** 117 Days and 18.2 Hours

**Adrián Cardín-Pereda, Daniel García-Sánchez, Itziar Álvarez-Iglesias, Jennifer Cabello-Sanz, Flor M Pérez-Campo**, Department of Molecular Biology, Instituto de Investigación Sanitaria Marqués de Valdecilla, Faculty of Medicine, University of Cantabria, Santander 39011, Cantabria, Spain

**Corresponding author:** Flor M Pérez-Campo, PhD, Assistant Professor, Senior Researcher, Department of Molecular Biology, Insituto de Investigación Sanitaria Marqués de Valdecilla, Faculty of Medicine, University of Cantabria, Avda Cardenal Herrera Oria S/N, Santander 39011, Cantabria, Spain. f.perezcampo@unican.es

## Abstract

***BACKGROUND***

Osteonecrosis of the femoral head (ONFH) is an ischaemic disorder often leading to collapse of the femoral head and severe hip dysfunction. Mesenchymal stem cells (MSCs) have a key role in bone repair, through their ability to differentiate into osteoblasts and their paracrine regulation of the bone microenvironment. While altered MSCs behaviour has been reported in some secondary forms of ONFH, the proliferative and differentiation programmes of MSCs in human idiopathic ONFH have not been previously characterized.

***AIM***

To compare the proliferative capacity, differentiation potential and nuclear factor kappa B (NF-κB) pathway activation of bone marrow MSCs (BM-MSCs) from idiopathic ONFH patients with those from osteoarthritis controls.

***METHODS***

Femoral heads were collected during total hip replacement surgeries. Idiopathic ONFH was defined by imaging and histological criteria. Secondary causes were excluded. BM-MSCs were isolated from trabecular bone cylinders and expanded to passage 2 prior characterizations. Proliferation was evaluated by 3-(4,5-dimethylthiazol-2-yl)-2,5-diphenyltetrazolium bromide assay at various seeding densities. Osteogenic potential was assessed by alkaline phosphatase activity, osteogenic gene expression (*RUNX2*, *ALPL*, *COL1A1* and *BGLAP*) and Alizarin Red staining. Adipogenesis was quantified by Oil Red O staining. Expression of NF-κB target genes (*IL6*, *NFKBIA*, *CCL2*) was analyzed by quantitative polymerase chain reaction.

***RESULTS***
Idiopathic ONFH MSCs exhibited significantly higher proliferation rates than osteoarthritis controls. However, they showed reduced alkaline phosphatase activity and osteogenic gene expression but paradoxically, increased mineralization, suggesting non-canonical mineral deposition mechanisms. These cells also display increased adipogenic differentiation. Importantly, ONFH-MSCs expressed higher, although non-significant levels of certain NF-κB target gene genes, consistent with an activated inflammatory state.

***CONCLUSION***
Human BM-MSCs from idiopathic ONFH display a paradoxical phenotype: Hyperproliferative yet osteogenically impaired with greater adipogenesis and activation of NF-κB signalling. This functional compromise and inflammatory bias may underline the failure of bone regeneration in ONFH, highlighting the need for therapies redirecting MSCs fate and modulating the bone marrow niche.

**Key Words:** Idiopathic osteonecrosis of the femoral head; Mesenchymal stem cells; Proliferation; Differentiation; Lineage specification; Adipogenesis; Osteogenesis



**Core Tip:** Directly harvested bone marrow mesenchymal stem cells from femoral heads of patients with idiopathic osteonecrosis show higher proliferation but reduced osteogenesis, increased adipogenesis and upregulated nuclear factor kappa B target genes relative to osteoarthritis controls. This hyperproliferative yet lineage-skewed phenotype offers a mechanistic link between cellular dysfunction and failed structural repair in osteonecrosis of the femoral head and supports the use of therapies that reprogramme mesenchymal stem cells fate and the bone marrow microenvironment.

**Citation:** Cardín-Pereda A, García-Sánchez D, Álvarez-Iglesias I, Cabello-Sanz J, Pérez-Campo FM. Altered lineage commitment of bone marrow mesenchymal stem cells in idiopathic osteonecrosis of the femoral head. *World J Orthop* 2025; 16(12): 113320
**URL:** https://www.wjgnet.com/2218-5836/full/v16/i12/113320.htm
**DOI:** https://dx.doi.org/10.5312/wjo.v16.i12.113320

## INTRODUCTION

Osteonecrosis of the femoral head (ONFH) is a progressive, disabling disease, difficult to treat, affecting young and middle-aged adults[1-3]. The progressive disruption of blood flow withing the bone leads to aseptic bone necrosis at the hip joint[4,5]. If left untreated, ONFH results in subchondral bone failure and collapse of the femoral head, triggering a secondary arthropathy and often requiring total hip arthroplasty (THA)[6]. Although ONFH can be secondary to well-known risk factors such as prolonged corticosteroid therapy[7,8], chronic alcohol intake[9,10] or haemoglobinopathies[11] a high percentage of cases are idiopathic, with no identifiable cause. Irrespective of aetiology, the osteonecrotic milieu is characterized by hypoxia, inflammatory signalling and altered mechanical loads that cooperatively impair bone remodelling and favour structural deterioration[3,12].

Mesenchymal stem cells (MSCs) are central to skeletal repair, not only through their ability to give rise to osteogenic cells, but also through their angiogenic/trophic signalling and immunomodulation, mediated by their paracrine action [13]. Defects in MSCs number, proliferative capacity and lineage commitment have been postulated as key contributors to the pathophysiology of certain types of ONFH[14,15]. In corticosterol-idinduced ONFH, several studies have described reduced MSCs proliferation and osteogenic potential accompanied by increased adipogenesis within the femoral head marrow[16,17]. However, whether these changes extend to idiopathic ONFH in humans remains insufficiently explored. Importantly, idiopathic disease may differ from steroidinduced disease in the intensity and wiring of hypoxic, inflammatory and metabolic cues that influence MSC behaviour[18].

Clarifying the cellular phenotype of MSCs in idiopathic ONFH is clinically relevant for at least three reasons. First, cell-based strategies, such as core decompression with MSCs augmentation, are increasingly considered for early stages of the disease, however the success of these techniques highly depends on the intrinsic quality and fate propensity of host MSCs. Second, a shift from osteogenesis towards adipogenesis can compromise trabecular integrity and mechanotransduction, accelerating the collapse of the femoral head. Third, identifying whether MSCs are proliferatively exhausted or conversely, hyperproliferative but functionally mis-specified will refine therapeutic targets: Promoting osteogenic fate, restraining adipogenesis, or correcting upstream niche signals. In this context, elucidating the molecular mechanisms underlying these phenotypic alterations becomes essential. Taken together, these considerations highlight the need to characterize the molecular mechanisms underlying the dysfunctional phenotype of MSCs in idiopathic ONFH.

Among the pathways of interest, nuclear factor kappa B (NF-κB) signalling has been implicated in multiple aspects of bone biology and MSCs function, including regulation of inflammation, senescence, and lineage commitment[19]. Dysregulated NF-κB activity has been described in pathological conditions such as osteoarthritis (OA) and ONFH, where it contributes to impaired regenerative potential and aberrant cytokine production[20]. Given its central role as a

transcriptional regulator of inflammatory mediators, the evaluation of NF-κB downstream gene expression would provide a functional readout of pathway activity in MSCs. Given the reported ability of NF-κB signalling to suppress osteogenesis while favouring adipogenic commitment, we hypothesised that NF-κB hyperactivation may contribute to the lineage bias observed in ONFH MSCs. In this study, we compared MSCs from ONFH and OA patients and found that ONFH MSCs display reduced osteogenic marker expression, a skew towards adipogenesis, and evidence of increased NF-κB pathway activation. These findings support the concept that MSC dysfunction in idiopathic ONFH is not due to proliferative exhaustion but rather to a misdirected differentiation programme probably driven by aberrant NF-κB activity.

## MATERIALS AND METHODS

### Study design and ethics

This was an observational basic study using specimens from THA. Idiopathic ONFH was diagnosed according to clinical and radiologic criteria at the treating centre; patients with secondary ONFH (*e.g.*, corticosteroid- or alcohol-associated) were excluded[4,21]. Histological confirmation of ONFH was done for all the specimens used in the study. Primary OA patients undergoing THA served as controls. All participants provided written informed consent. The protocol was approved by the Medical Ethics Committee of Cantabria Clinical Research, approval No. 2018.014 and complied with the Declaration of Helsinki.

### Patients and specimens

Only patients complying with our stringent selection criteria were used in the study. All secondary ONFH were excluded: Systemic glucocorticoids and/or bisphosphonate treatment history, past or present heavy alcohol consumption, hip trauma or radiation history, storage disorders, pancreatitis, hemoglobinopathies or dysbarism history. Femoral heads of patients were collected intraoperatively and processed under sterile conditions as previously described [22]. The diagnostic procedures combining advanced imaging and histological confirmation have been previously published[4]. Cases lacking a certified report from a radiologist or that were not confirmed by histology studies were excluded. All samples were classified according to these methods, ensuring reproducibility and the highest level of diagnostic accuracy. In total, 60 femoral heads were initially enrolled (26 idiopathic ONFH and 34 OA). Given the known challenges in maintaining MSCs cultures for long periods of time without loss of replicative potential and to avoid bias, MSCs cultures were only expanded to passage 2 (P2) prior to test their proliferation or differentiation capacity. For proliferation and gene expression analyses, 10 ONFH and 10 OA MSC lines were included. For osteogenic differentiation, 6 ONFH and 6 OA lines were available; for adipogenesis, 4 ONFH and 7 OA lines. For clarity, a sample flow is provided in Supplementary Figure 1.

Baseline demographic and clinical data of the idiopathic ONFH cohort have been reported in detail in previous publications from the same recruitment pipeline and Institutional Review Board protocol, No. 2018.014[4,21]. In these studies, ONFH patients had a mean age of 66.46 ± 11.07 years, and comorbidities included overweight/obesity (61%), smoking (53%), hypertension (50%), dyslipidemia (34%), and diabetes (15%). Importantly, ONFH and OA groups did not differ significantly in age within the analyzed set (65.9 ± 12.6 years *vs* 63.8 ± 10.9 years; $P = 0.263$). These data support the comparability of our groups and avoid redundancy in the present manuscript.

### MSC isolation and expansion

Bone samples were isolated from the macroscopically affected areas of the femoral head specimens. Bone cylinders were extracted from the sample with the help of a trephine. Trabecular bone cylinders were washed thoroughly to release marrow cells. Cell suspension was then plated on tissue culture plates to allow adherence of MSCs. Cells were maintained in Mesenpro RS Media (Ref. 12746012, Gibo, Thermo Fischer Scientific, Waltham, MA, United States), Supplemented with 1% of Glutamax (Ref. 35050038, Gibco, Thermo Fisher Scientific, Waltham, MA, United States) in a humidified 5% $CO_2$ atmosphere. Only cells at P2 were used for subsequent experiments. Morphology and growth were monitored routinely.

### MSC characterization

MSCs were defined by plastic adherence and characterized Immunophenotypically by flow cytometry (CD73/CD90/CD105 positive; CD34/CD45) as previously described[22]. Representative gating plots illustrating the $CD73^+/CD90^+/CD105^+/CD34^-/CD45^-$ immunophenotype are provided in Supplementary Figure 1 to confirm compliance with the International Society for Cell and Gene Therapy criteria.

### Proliferation assay (3-(4,5-dimethylthiazol-2-yl)-2,5-diphenyltetrazolium bromide)

Cells were seeded in 96well plates at four densities (*e.g.*, 200 cells/well, 400 cells/well, 800 cells/well and 1000 cells/well) in quadruplicate per condition. We measured metabolic activity as a proxy for proliferation on days 1, 3, 5 and 7 using 3-(4,5-dimethylthiazol-2-yl)-2,5-diphenyltetrazolium bromide (Ref. 475989, Sigma-Aldrich, Burlington, MA, United States) (0.5 mg/mL; 4 hours incubation). Formazan crystals were solubilized with 2 propanol and absorbance read at 570 nm.

### Osteogenic and adipogenic differentiation

To induce osteogenic differentiation primary human MSCs were plated at 20.000 cells/cm², allowing them to attach

overnight. Osteogenic differentiation was induced by culturing confluent MSCs for 20 days with Dulbecco's modified Eagle medium (10% fetal bovine serum, 1% Pen/Strep) supplemented with 50 µmol/L ascorbic acid (Ref. A4034, Sigma-Aldrich, Burlington, MA, United States), 10 mmol/L β-Glycerophosphate (Ref. G9422, Sigma-Aldrich, Burlington, MA, United States) and 0,1 µmol/L dexamethasone (Ref. D4092, Sigma-Aldrich, Burlington, MA, United States) with medium changes every 2-3 days.

For adipogenic differentiation, MSCs were induced for 14–21 days in Dulbecco's modified Eagle medium (10% fetal bovine serum, 1% Pen/Strep) supplemented with 1 µmol/L Dexamethasone, 2 µmol/L Rosiglitazone (Ref. R2408, Sigma-Aldrich, Burlington, MA, United States), 5 µg/mL Insulin (Ref. I26343, Sigma-Aldrich, Burlington, MA, United States) and 0,5 mmol/L 3-Isobutyl-1-methylxanthine (Ref. I5879, Sigma-Aldrich, Burlington, MA, United States).

### *RNA extraction and gene expression analysis*

mRNA was isolated from cell cultures, after washing the cells twice with phosphate-buffered saline (PBS) and collecting them with TRIzol reagent (Invitrogen, Waltham, MA, United States). RNA was extracted from cell cultures, and cDNA conversion was performed as previously described[23]. Gene expression analysis was carried out by real-time quantitative polymerase chain reaction (qPCR). Taqman assays were used for this analysis (ThermoFisher Scientific). Assays probes were as follows: *GAPDH* (Hs99999905_m1), *RUNX2* (Hs00231692_m1), *ALPL* (Hs00758162_m1), *BGLAP* (Hs01587814_g1), *PPARg* (Hs01115513_m1), *LPL* (Hs00173425_m1), *IL6* (Hs00174131_m1), *TNFa* (Hs00174128_m1) and *NFKBIA* (Hs00355671_g1). Relative gene expression was quantified using the comparative Ct method. Expression levels of target genes were normalized to the housekeeping gene glyceraldehyde-3-phosphate dehydrogenase, detected with a TaqMan probe (Hs99999905_m1, Applied Biosystems). Results are presented as relative expression values normalized to glyceraldehyde-3-phosphate dehydrogenase.

### *Alizarin Red and Oil Red stainings and quantification*

For these analysis all cultures were initiated at identical confluence and verified visually before staining to ensure comparable cell density. At the endpoint, cells were fixed with 70% ethanol for 1 hour, washed, stained with 500 µL Alizarin Red (Ref. A5533, Sigma-Aldrich, Burlington, MA, United States) solution (pH 4.2) for 15 minutes, and then washed again before imaging each well. Alizarin Red quantification was performed using a modification of a previously described method[24]. Cells were incubated with 10% acetic acid, detached, and collected into tubes. After vortexing and centrifugation, samples were heated at 85 °C, cooled on ice, and centrifuged again. The supernatant was mixed with 10% NaOH, vortexed, briefly centrifuged, and transferred to a 96-well plate for absorbance measurement at 405 nm.

For Oil Red staining, cells were fixed with 10% formaldehyde (5 minutes + 1 hour) after PBS washes, then rinsed with 60% isopropanol and air-dried. Oil Red (Ref. ht501128, Sigma-Aldrich, Burlington, MA, United States) solution was applied for 10 minutes at room temperature, followed by three washes with distilled water. Quantification was performed following a previously described protocol[25]. In brief, wells were washed two times with distilled water. After the washes 200 µL of 100% isopropanol was added to the wells. Plates were then incubated at room temperature for 10 minutes with gentle shaking. After this time the isopropanol was recovered from the wells and the 200 µL were deposited in 2 wells of a 96 well plate (100 µL per well). Absorbance of the samples was read at 510 nm.

For both Alizarin Red and Oil Red stainings, homogeneous confluence was verified before staining and three different technical replicates were done for each of the samples to minimize variability.

### *Alkaline phosphatase activity*

Cells induced towards osteogenic differentiation were rinsed twice with PBS and lysed by scraping in 0.05% Triton X-100 (Merck KGaA, Darmstadt, Germany). The lysates were subjected to three sonication cycles (30 seconds on/30 seconds off) at 4 °C, followed by centrifugation to obtain the supernatant. Samples were stored at -80 °C until analysis. Alkaline phosphatase activity was determined as described previously[26], and absorbance was recorded with an Eon Microplate Spectrophotometer (BioTek, Winooski, VT, United States). Three different technical replicates were done for each of the samples to minimize variability.

### *Sample sizes and data handling*

Final sample sizes reflected the number of independent MSCs lines that reached the required passage and quality control for each assay: Proliferation and qPCR analysis (ONFH $n$ = 10, OA $n$ = 10), osteogenesis (ONFH $n$ = 6, OA $n$ = 6) and adipogenesis (ONFH $n$ = 4, OA $n$ = 7). A sample flow graph is shown in Supplementary Figure 1. Each line was treated as a biological replicate. Three technical replicates (*e.g.*, wells per condition) were averaged to obtain one value per line and endpoint.

### *Statistical analysis*

Data are presented as mean ± SEM unless otherwise specified. Comparisons between two groups were performed using either Student's $t$ test (for normally distributed data) or Mann-Whitney $U$ test (for non-parametric data). Proliferation data were analyzed using generalized estimating equations (GEE) with a Gaussian distribution and identity link, accounting for repeated measures within patients. Separate models were fitted for each seeding density (200 cells, 400 cells, 800 cells, and 1000 cells per well), including group (OA *vs* ONFH), day (categorical), and their interaction (group × day) as fixed effects. Patient identifier was specified as the clustering variable with an exchangeable correlation structure. Estimated marginal means (EMMs) with 95% confidence intervals were derived for each group and day. Marginal contrasts were computed within the GEE framework to test differences between OA and ONFH at each time point. In addition, a global model was fitted including all seeding densities with adjustment for cell number, and EMMs were

averaged across conditions. Statistical significance was set at $P < 0.05$. All analyses were performed in Python.

## RESULTS

### Patient cohort and MSC yields

Of 60 femoral heads processed, primary MSC expansion to experimental passages was feasible only in a subset (20 ONFH and 30 OA) owing to reduced cell yield from necrotic areas. Out of all the lines obtained only 10 OA-MSCs and 10 ONFH-MSCs that fulfilled strict inclusion and diagnosis criteria[21] were chosen to perform the proliferation and qPCR analysis and for further expansion. Differentiation assays required a larger number of cells than proliferation analysis and at least three technical replicates are necessary to ensure consistency of the results, thus, further expansion to P2 was required. Consequently, the number of patient-derived MSCs samples included in the differentiation analysis was lower, as these cells were difficult to expand in culture without triggering early entry into cellular senescence (Table 1). In total, for differentiation assays, availability was ONFH $n = 6$/OA $n = 6$ (osteogenesis) and ONFH $n = 4$/OA $n = 7$ (adipogenesis). Analyses of osteogenic potential were prioritized over adipogenic differentiation, and the lower number of samples available for osteogenesis reflects the limited cell yield obtained at P2. The difference in sample numbers (7 OA for adipogenesis and 6 ONFH for osteogenesis) was due to contamination of one ONFH osteogenic differentiation culture. Where demographic information was available, groups were generally comparable in age range typical of THA populations.

### ONFH MSCs exhibit enhanced proliferation compared with OA controls

To account for the influence of initial confluence on proliferation capacity, MSCs were seeded at four different starting densities in quadruplicate for each experimental group. For each density a GEE model including group (OA *vs* ONFH), day (1, 3, 5, 7) and the group × day interaction was fitted, clustering by patient, and EMMs with 95% confidence intervals were estimated. Group differences at each time point were assessed by marginal contrasts within the GEE. This approach allowed correction for seeding density effects and improved the reliability of proliferation measurements. Across densities, both OA and ONFH populations exhibited increasing absorbance over time. In the global GEE (all densities combined, adjusted for seeding density), ONFH samples displayed consistently higher EMM absorbance than OA. Marginal contrasts indicated significant ONFH > OA differences at day 5 and day 7 ($P < 0.05$), while differences at day 1 and day 3 were not significant. When models were fitted separately by seeding density, the same general trend was observed (ONFH ≥ OA), though the time points reaching statistical significance varied with density because of differences in variance and sample sizes (Figure 1). These results support a time-dependent group effect (group × day interaction) with ONFH-derived MSCs showing a hyperproliferative profile relative to OA controls, particularly at intermediate time points.

### Osteogenic differentiation is attenuated in ONFH MSCs

Following 20 days of osteogenic induction, MSCs were assessed by ALP activity, expression of key osteogenic markers and mineralization. While no significant differences were observed in the early markers *RUNX2* and *ALPL*, ONFH MSCs exhibited significantly lower expression of the late-stage markers osteocalcin (*BGLAP*) and *COL1A1*, associated with extracellular matrix production, compared with OA controls (Figure 2). Importantly ONFH MSCs displayed reduced ALP activity normalized to protein content relative to OA controls. Paradoxically, Alizarin Red staining showed increased calcium deposition in ONFH cultures, supported by higher dye extraction values (Figure 2).

### Adipogenic differentiation is increased in ONFH MSCs

In adipogenic conditions, ONFH MSCs express higher levels of key adipogenic markers such as *PPARg* and *LPL*, than the control samples. Importantly, the idiopathic ONFH MSCs also accumulated more lipid droplets, exhibiting higher Oil Red O extraction compared with OA MSCs. These clearly indicates a shift towards adipogenic lineage allocation (Figure 3). This adipogenic propensity complements the reduced osteogenesis observed above and points to a lineage bias in ONFH MSCs.

### Differential expression of NF-κB target genes in MSCs from ONFH and OA

To further characterize NF-κB activity in MSCs from ONFH and OA, we assessed the expression of three canonical NF-κB target genes: Interleukin (*IL*)-*6*, *NFKBIA*, and tumor necrosis factor α (*TNFα*) (Figure 4). These genes were chosen because they represent different facets of NF-κB-mediated responses: *IL6* as a prototypical pro-inflammatory cytokine, *NFKBIA* as a direct negative feedback regulator of NF-κB signalling, and *TNFα* as a central cytokine classically induced by NF-κB in immune cells[27-29]. Quantitative PCR analysis revealed a significant upregulation of *IL6* and *NFKBIA* in ONFH-MSCs compared with OA-MSCs, whereas *TNFα* expression did not differ significantly between groups.

## DISCUSSION

Bone marrow MSCs are characterized by a notable differentiation potential and an important paracrine activity, which are key to regulate the function of other cells in the bone marrow microenvironment. Thus, these cells are central in mediating bone repair in osteonecrosis and other bone pathologies. Although several studies report reduced MSCs

**Table 1 Yield of mesenchymal stem cells obtained from femoral head samples, *n* (%)**

| Number of samples collected | Samples collected and processed | Progression to P1 | Progression to P2 |
|---|---|---|---|
| **Number of samples (osteoarthritis controls)** | 34 | 30 (88) | 7 (25) |
| **Number of samples (ONFH)** | 26 | 20 (79) | 9 (46) |

Values rounded to nearest whole percent. P1, P2: Passages 1 and 2 (transfer to a new flask); ONFH: Osteonecrosis of the femoral head.

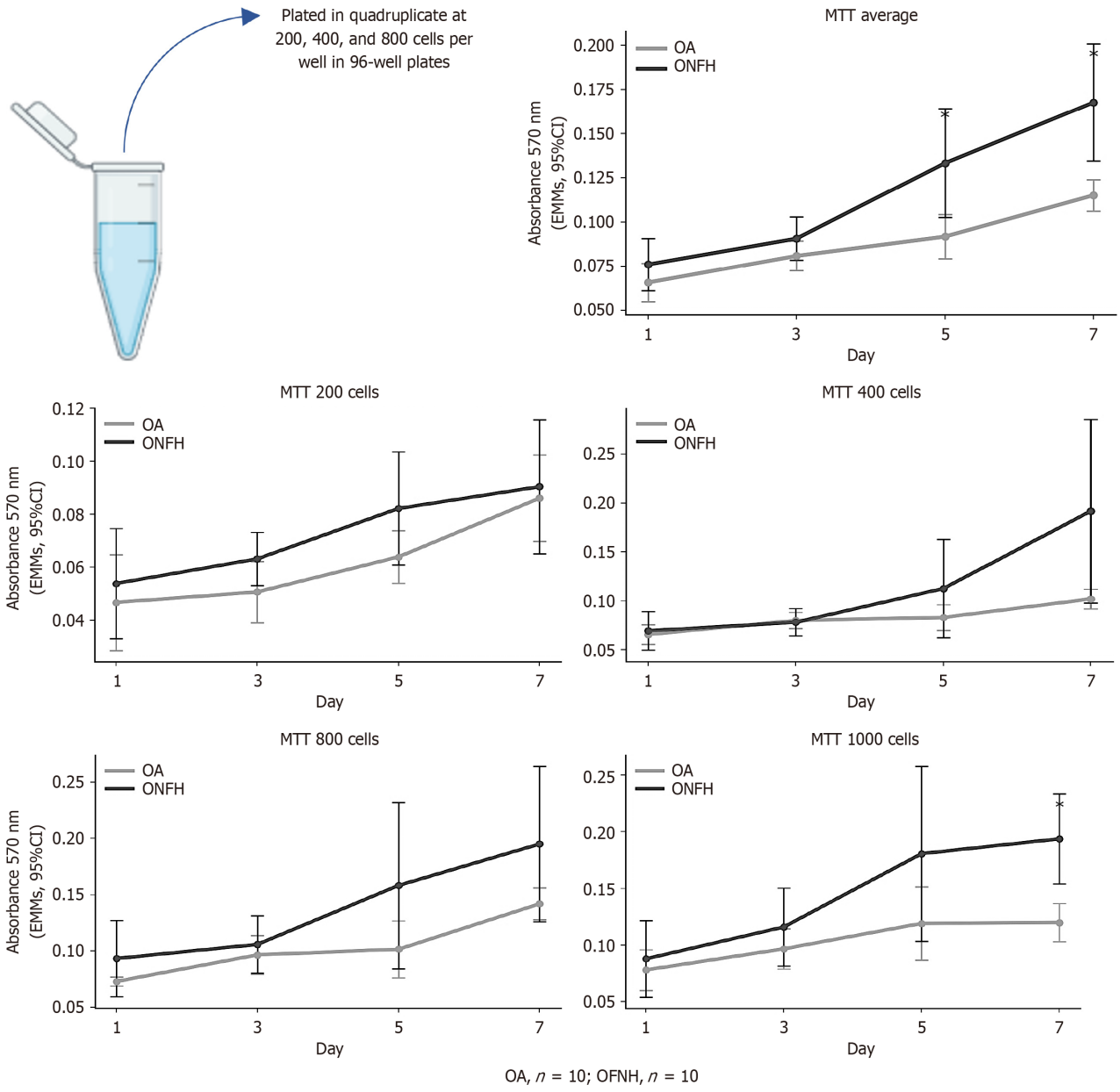


**Figure 1 Proliferation of mesenchymal stem cells assessed by 3-(4,5-dimethylthiazol-2-yl)-2,5-diphenyltetrazolium bromide assay.** Absorbance at 570 nm was measured in mesenchymal stem cells derived from patients with osteonecrosis of the femoral head (black line) and osteoarthritis of the hip (gray line) at different culture time points (days 1, 3, 5, and 7). Cells were plated in quadruplicate at 200 cells, 400 cells, 800 cells, or 1000 cells per well, as shown in the lower panels, and a global analysis averaging across all seeding densities is presented in the upper panel. Values represent estimated marginal means with 95% confidence intervals obtained from generalized estimating equation models with patient identifier as clustering variable and an exchangeable correlation structure. Asterisks denote significant differences between groups at the corresponding time point ($P < 0.05$). Biological replicates: Osteoarthritis $n = 10$, osteonecrosis of the femoral head $n = 10$. CI: Confidence interval; EMMs: Estimated marginal means; OA: Osteoarthritis; ONFH: Osteonecrosis of the femoral head; MTT: 3-(4,5-dimethylthiazol-2-yl)-2,5-diphenyltetrazolium bromide.

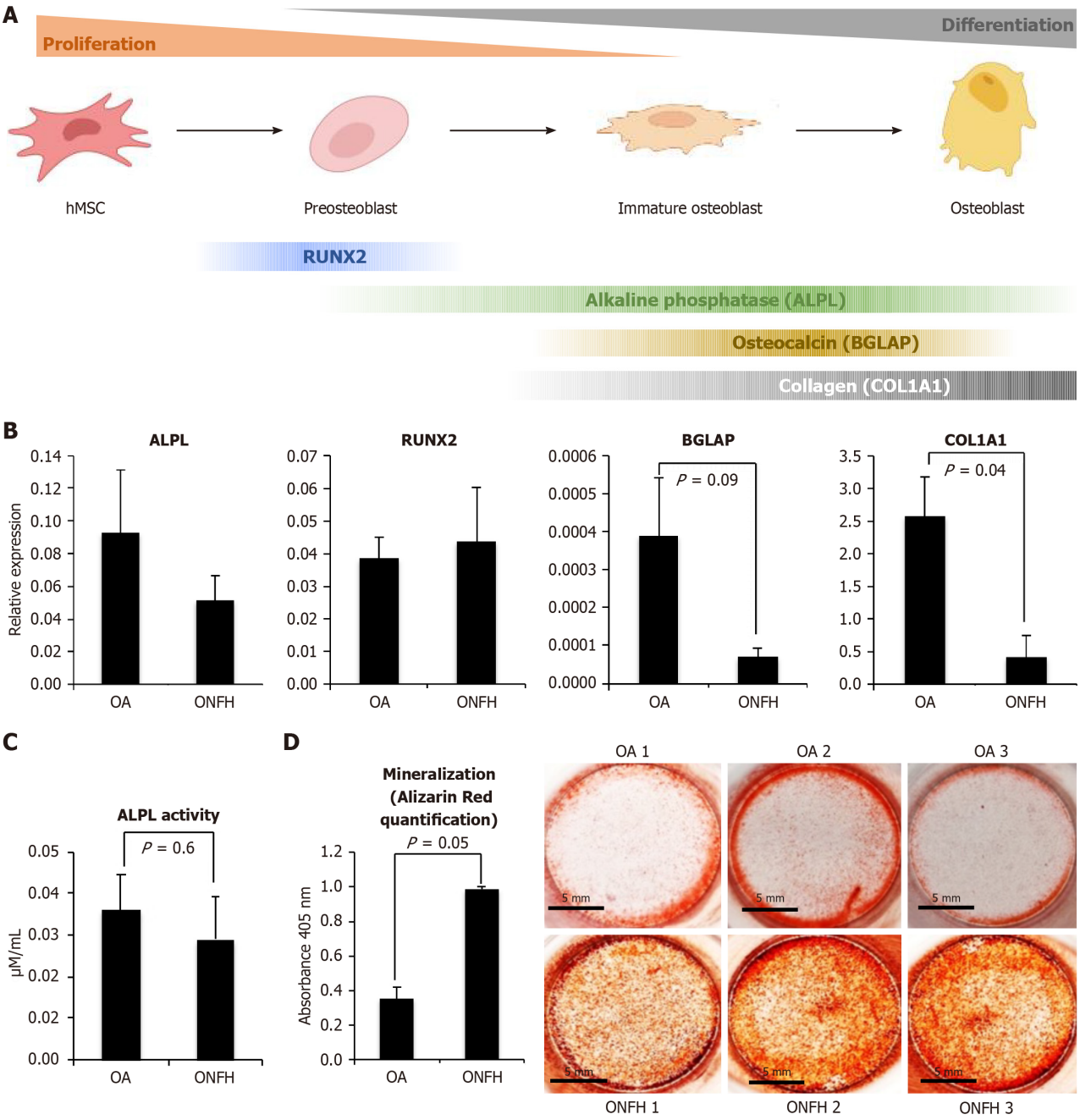


**Figure 2 Osteogenic differentiation of mesenchymal stem cells derived from osteoarthritis and osteonecrosis of the femoral head patients.** Images shown on the right are representative of 6 independent samples in each group [osteoarthritis (OA), *n* = 6; osteonecrosis of the femoral head (ONFH), *n* = 6]. Identical cell confluence was verified prior to perform Alizarin Red or Oil Red stainings. Despite reduced osteogenic marker expression, ONFH MSCs showed increased Alizarin Red signal, consistent with a paradoxical mineralization phenotype Graphs display the mean ± SEM for each group Statistical significance is indicated by *P* values in the graphs. A: Expression of the different osteogenic markers analyzed along osteogenic differentiation; B: At day 20 of osteogenic induction, gene expression levels of *RUNX2*, *ALPL*, *COL1A1*, and *BGLAP* were quantified by quantitative polymerase chain reaction (ONFH, *n* = 10; OA, *n* = 10); C: *ALPL* gene expression and enzymatic activity assessed at day 20 under osteogenic conditions to confirm early differentiation events (ONFH, *n* = 6; OA, *n* = 6); D: Mineralization capacity was evaluated by measuring the intensity of Alizarin Red staining after 20 days of induction. OA: Osteoarthritis; ONFH: Osteonecrosis of the femoral head. Created with BioRender.com.

activity and number, particularly in steroid-induced ONFH[16,17,30,31], our idiopathic cases showed preserved or even increased proliferation with impaired ostegenic differentiation. Unlike previous studies where ONFH diagnosis relied primarily on imaging criteria, in our work patient samples were stringently verified using advanced imaging and histological assessment, considered the gold standard for ONFH diagnosis[4]. Given the diagnostic challenges inherent to idiopathic ONFH, this rigorous confirmation substantially strengthens the reliability of our findings. In relation to the proliferation assays, we acknowledge that the 3-(4,5-dimethylthiazol-2-yl)-2,5-diphenyltetrazolium bromide assay does not directly measure cell division but rather mitochondrial metabolic activity. However, it is widely recognized and accepted as a reliable proxy for MSCs proliferation in the field, correlating well with other proliferation metrics, such as BrdU incorporation and cell doubling time, when applied to MSC cultures[32-34].

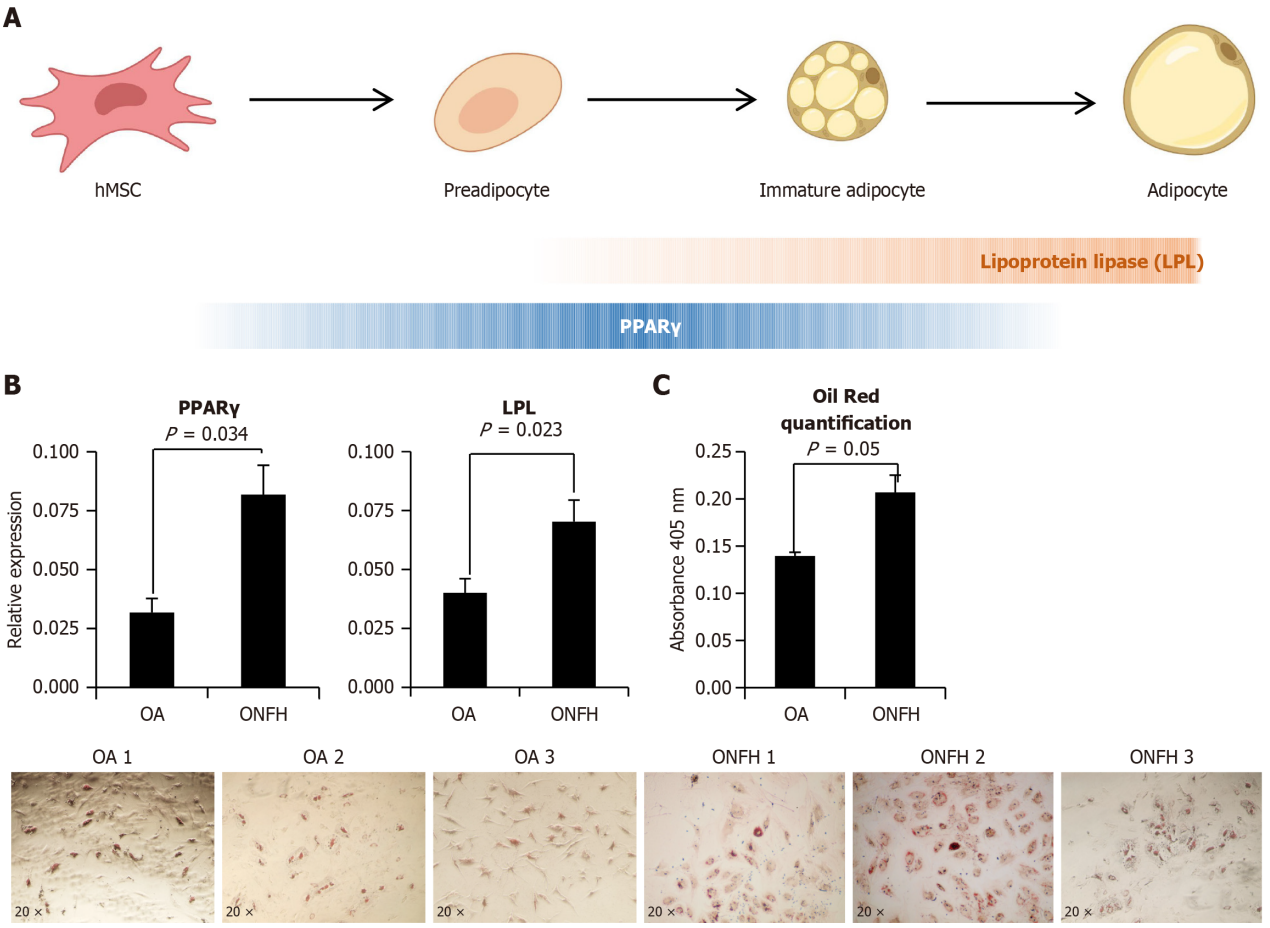


**Figure 3 Adipogenic differentiation of bone-marrow mesenchymal stem cells from osteoarthritis and osteonecrosis of the femoral head patients.** Quantification of lipid accumulation was performed by absorbance at 405 nm in osteoarthritis and osteonecrosis of the femoral head mesenchymal stem cell cultures, and light microscopy images of Oil Red O staining after 20 days of induction are shown. Images are representative of 6 independent samples the samples in each group (osteoarthritis, *n* = 7; osteonecrosis of the femoral head, *n* = 4). Data represent the mean of the samples analyzed in each group and are shown as mean ± SEM; *P* values are indicated on the graphs. A: Schematic of mesenchymal stem cell lineage allocation towards adipocytes; B: Expression of adipogenic regulators after induction; relative mRNA levels of peroxisome proliferator-activated receptor gamma and lipoprotein lipase; C: Adipogenic differentiation assessed by Oil Red O staining. OA: Osteoarthritis; ONFH: Osteonecrosis of the femoral head; LPL: Lipoprotein lipase; PPARγ: Peroxisome proliferator-activated receptor gamma; hMSC: Human mesenchymal stem cells. Created with BioRender.com.

The increase in proliferation observed in our study may represent a compensatory response to the stressful ischaemic bone marrow niche, characterized by chronic hypoxia and inflammation, since these conditions are known to activate signalling pathways such as hypoxia-inducible factor 1-alpha and NF-kB, that support survival and inflammation[19,35]. Importantly, in this case a higher proliferative rate does not necessarily imply a greater regenerative capacity, as ONFH MSCs show lineage defects that limit their contribution to bone homeostasis. Our data revealed a clear increase in adipogenic potential in idiopathic ONFH MSCs which correlates with a lower expression of late osteogenic markers. This pattern fits the previously described reciprocal relationship between adipogenesis and osteogenesis, the so called "adipogenic-osteogenic switch", where commitment to one lineage is done at the expense of, or supresses the other[36]. Mechanistically, activation of *PPARg*, a master regulator of adipogenesis, antagonises *RUNX2*-driven osteogenesis through competition for key epigenetic cofactors[37]. In ONFH, chronic hypoxia and inflammatory cues are possible drivers of the *PPARg* activation seen in our study, explaining the observed enhanced adipogenesis. Importantly, mechanical unloading in necrotic bone regions may actually reinforce this bias, further inclining the balance away from bone formation[38].

In our work, the reduced osteogenic differentiation was evidenced by the down-regulation of late osteogenic markers *BGLAP* and *COL1A1*, which are essential for osteoblast maturation and the formation of a functional matrix. This was accompanied by lower alkaline phosphate activity, a key early driver of bone mineralization[39]. Such deficits have been linked to disturbances in bone morphogenetic protein and Wnt/b-catenin signalling, as reported in steroid-induced ONFH models. Paradoxically, our *in vitro* assays revealed increased mineralization in idiopathic ONFH MSCs compared with the control group despite the downregulation of osteogenic markers such as *BGLAP* and *COL1A1* and the non-significant downward trends in *ALPL* expression and activity. Since mineralization represents the terminal hydroxyapatite-deposition step, this discrepancy suggests the involvement of alternative non-canonical mineralizing mechanisms. In this sense, hypoxia and inflammation have been shown to induce ectopic mineralization *via* cytokines such as TNFα and IL6, which drive pathological calcification in other contexts[40] and act in part *via* NF-kB signalling.

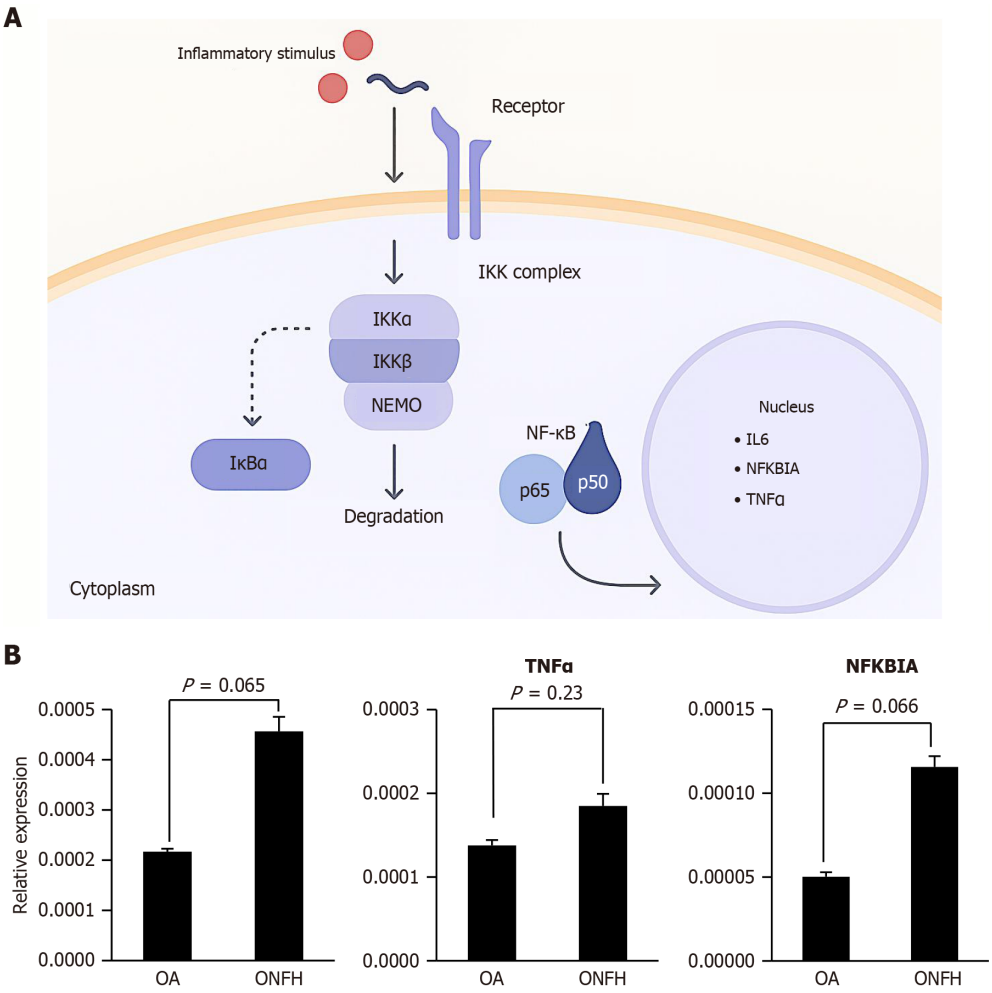


**Figure 4 Nuclear factor kappa B pathway activation and target gene expression in mesenchymal stem cells from osteoarthritis and osteonecrosis of the femoral head.** Data are presented as mean ± SEM. Statistical analysis was performed using Student's *t*-test; *P* values are indicated. A: Schematic representation of nuclear factor kappa B signalling under inflammatory stimulation. Upon receptor activation, the inhibitor of nuclear factor kappa-B kinase complex phosphorylates the inhibitor of nuclear factor kappa B alpha, leading to its degradation and release of the nuclear factor kappa B p65/p50 dimer, which translocates to the nucleus and regulates the transcription of target genes such as *IL6*, *NFKBIA*, and *TNFα*; B: Relative mRNA expression levels of interleukin 6, tumor necrosis factor alpha, and nuclear factor kappa B inhibitor alpha in mesenchymal stem cells derived from osteoarthritis ($n$ = 10) and osteonecrosis of the femoral head ($n$ = 10) patients, measured by quantitative polymerase chain reaction. OA: Osteoarthritis; ONFH: Osteonecrosis of the femoral head; NF-κB: Nuclear factor kappa B; IκBα: Inhibitor of nuclear factor kappa-B alpha; IKK: Inhibitor of nuclear factor kappa-B kinase; NEMO: Nuclear factor kappa B essential modulator; IL6: Interleukin 6; NFKBIA: Nuclear factor kappa B inhibitor alpha; TNFα: Tumour necrosis factor alpha.

Although no statistically significant differences were detected in the expression levels of the three NF-κB targets analyzed, the expression profile of ONFH-MSCs suggested a tendency towards increased *IL6* and *NFKBIA* levels. The absence of significance may be partly explained by the relatively low number of biological samples available and by the inherently low expression levels of these markers, both of which reduce statistical power. Prior studies have shown that *IL6* contributes to the inflammatory phenotype of MSCs and modulates their immunoregulatory properties. Moreover, NF-κB signalling has been described as a negative regulator of MSCs osteogenic differentiation[41], supporting the idea that even subtle pathway activation may impair bone-forming capacity. In contrast, TNFα expression seemed to remain unchanged, consistent with its predominant regulation in immune cells rather than MSCs[42]. Thus, the observed increase in mineral deposition despite reduced expression of key osteogenic markers would suggests that this mineralization does not reflect a canonical osteogenic programme. Instead, it likely represents a non-physiological, inflammation-driven process. This apparent paradox between marker down-regulation and enhanced Alizarin Red signal supports the view that ONFH-MSC mineralization may result from inflammation-driven calcification rather than true osteogenic maturation.

Studies have shown that chronic or intermittent hypoxia impairs osteogenesis and enhances adipogenesis in bone marrow MSCs showing reduced expression of osteogenic genes and increased lipid accumulation under these conditions [43]. A recent review summarizes that hypoxia-induced osteogenesis is context-dependent: Mild hypoxia may in some settings maintain stemness or modestly support proliferation, but prolonged or severe hypoxia tends to suppress osteogenic differentiation while favouring adipogenic commitment[44]. These observations fit well with our own findings: MSCs from idiopathic ONFH proliferate but exhibit reduced osteogenesis and a shift towards adipogenesis. They also highlight hypoxia as a promising avenue for future research in ONFH. Although in the present study we were

unable to address the direct impact of hypoxia on ONFH MSCs due to the lack of viable material, we acknowledge this as a highly relevant question. Future studies specifically designed to evaluate how hypoxic conditions influence the ONFH niche will be essential to complement our current findings and to better understand the mechanisms driving MSC dysfunction in this disease.

The lineage misallocation observed in MSCs from idiopathic ONFH has important clinical consequences. Bone homeostasis relies on a delicate equilibrium between osteoblasts and adipocytes, and when MSCs are diverted towards fat, bone repair is inevitably compromised. Similar mechanisms have been described in osteoporosis, where marrow fat accumulation is linked to reduced osteogenesis[45]. From a therapeutic standpoint, these findings encourage strategies that actively drive MSCs towards the bone-forming pathways. Potential approaches would include stimulation of Wnt/β-catenin and bone morphogenetic protein signaling to enhance osteoblast commitment and reduce adipogenesis. In fact, our group has shown that activation of these osteogenic pathways through transient silencing of key inhibitors significantly increases MSCs osteogenic potential[23] and bone regeneration in murine models of post-menopausal osteoporosis[46].

Our results highlight that idiopathic and steroid-induced ONFH exhibit distinct biological profiles, supporting the view that ONFH is not a single disease but a family of conditions with different triggers. In idiopathic ONFH, MSCs retain proliferative capacity but display impaired osteogenic differentiation, suggesting that the problem is not depletion but misallocation of lineage fate. This distinction is clinically relevant.

Patients with idiopathic ONFH may still harbor an abundant progenitor pool that could be leveraged therapeutically. Clinical evidence indicates that combining core decompression with stem cell therapy yields superior outcomes, such as lower collapse and arthroplasty conversion rates, even when cell number varies per protocol[47]. Moreover, in a large cohort of 908 ONFH cases, Hernigou *et al*[48], in 2024 demonstrated that efficacy is influenced by factors beyond cell count, highlighting the role of osteogenic competence in regenerative success[48]. Additionally, in sickle-cell disease patients with early ONFH, implantation of bone marrow progenitor-enriched cells maintained femoral head integrity and functional outcomes over a 5-year period, suggesting that cell quality can be decisive[49].

By analyzing MSC proliferation, osteogenesis, and adipogenesis directly from femoral heads, we captured the effects of the disease microenvironment with strong clinical relevance. While sample size was limited, the diagnostic certainty of our cohort was maximized by confirmation through both imaging and histology, ensuring the highest accuracy. Overall, our findings challenge the idea that idiopathic ONFH is simply a matter of stem cell depletion. Instead, they reveal a qualitative defect in MSC fate decisions, underscoring the need for patient stratification and therapies that not only preserve MSC survival but also restore their osteogenic potential.

Our work is not without limitations. The number of idiopathic ONFH MSCs lines that could be expanded and analyzed was necessarily small, which reflects both the rarity of strictly histology-confirmed idiopathic cases and the technical challenges of propagating primary MSCs. In addition, OA samples were used as the comparator group rather than healthy femoral heads; while this is a pragmatic and widely adopted choice, it is not a perfect control. It was also not possible to reproduce the hypoxic microenvironment or to perform *in vivo* bone formation assays within the scope of this study. Finally, the limited number of lines prevented stratified or adjusted analyses for comorbidities. We believe, however, that these constraints are balanced by the rigorous diagnostic confirmation of idiopathic ONFH and using complementary functional and molecular assays, which together provide confidence in the robustness of our conclusions.

## CONCLUSION

BM-MSCs from idiopathic ONFH display a paradox of enhanced proliferation with reduced osteogenesis and increased adipogenesis relative to OA controls. This lineage skewed, functionally compromised state likely contributes to failed bone regeneration in idiopathic ONFH and highlights the need for fate directed and niche-modulating therapies.

## ACKNOWLEDGEMENTS

The authors thank the orthopaedic surgery team at the Hospital Universitario Marqués de Valdecilla (Cantabria, Spain) and for assistance with specimen collection.

## FOOTNOTES

**Author contributions:** Cardín-Pereda A was responsible for investigation; Cardín-Pereda A and García-Sánchez D were responsible for methodology; Cardín-Pereda A and Pérez-Campo FM were responsible for conceptualization; Cardín-Pereda A, García-Sánchez D, Álvarez-Iglesias I, and Cabello-Sanz J were responsible for formal analysis; Pérez-Campo FM was responsible for resources; Cardín-Pereda A and Álvarez-Iglesias I were responsible for writing of the original draft; Cardín-Pereda A, García-Sánchez D, Álvarez-Iglesias I, Cabello-Sanz J, and Pérez-Campo FM were responsible for writing review and editing; Pérez-Campo FM was responsible for supervision; and all authors thoroughly reviewed and endorsed the final manuscript.

**Institutional review board statement:** This study was approved by the Medical Ethics Committee of Cantabria Clinical Research, approval No. 2018.014.

**Conflict-of-interest statement:** All the authors report no relevant conflicts of interest for this article.

**Data sharing statement:** Anonymized datasets generated and analyzed during this study are available from the corresponding author upon reasonable request. Individual-level patient data cannot be shared due to privacy regulations.



**Country of origin:** Spain

**ORCID number:** Adrián Cardín-Pereda 0000-0002-6431-6077; Daniel García-Sánchez 0000-0002-1754-9185; Itziar Álvarez-Iglesias 0009-0002-6830-2286; Jennifer Cabello-Sanz 0009-0007-5969-588X; Flor M Pérez-Campo 0000-0002-9872-7990.

**S-Editor:** Bai Y
**L-Editor:** A
**P-Editor:** Lei YY

## REFERENCES

1 **Chen Y**, Miao Y, Liu K, Xue F, Zhu B, Zhang C, Li G. Evolutionary course of the femoral head osteonecrosis: Histopathological - radiologic characteristics and clinical staging systems. *J Orthop Translat* 2022; **32**: 28-40 [*RCA*] [PMID: 35591937 DOI: 10.1016/j.jot.2021.07.004] [Full Text] [Full Text(PDF)]
2 **Gagala J**, Buraczynska M, Mazurkiewicz T, Ksiazek A. Prevalence of genetic risk factors related with thrombophilia and hypofibrinolysis in patients with osteonecrosis of the femoral head in Poland. *BMC Musculoskelet Disord* 2013; **14**: 264 [*RCA*] [PMID: 24025446 DOI: 10.1186/1471-2474-14-264] [FullText] [Full Text(PDF)]
3 **Moya-Angeler J**, Gianakos AL, Villa JC, Ni A, Lane JM. Current concepts on osteonecrosis of the femoral head. *World J Orthop* 2015; **6**: 590-601 [*RCA*] [PMID: 26396935 DOI: 10.5312/wjo.v6.i8.590] [FullText] [Full Text(PDF)]
4 **Cardín-Pereda A**, García-Sánchez D, Terán-Villagrá N, Alfonso-Fernández A, Fakkas M, Garcés-Zarzalejo C, Pérez-Campo FM. Osteonecrosis of the Femoral Head: A Multidisciplinary Approach in Diagnostic Accuracy. *Diagnostics (Basel)* 2022; **12**: 1731 [*RCA*] [PMID: 35885636 DOI: 10.3390/diagnostics12071731] [FullText] [Full Text(PDF)]
5 **Woerner M**, Voelkl K, Bliemel C, Ferner F, Weber M, Renkawitz T, Grifka J, Craiovan B. Comparison of two joint-preserving treatments for osteonecrosis of the femoral head: core decompression and core decompression with additional cancellous bone grafting. *J Int Med Res* 2023; **51**: 3000605231190453 [*RCA*] [PMID: 37585739 DOI: 10.1177/03000605231190453] [FullText]
6 **Mont MA**, Zywiel MG, Marker DR, McGrath MS, Delanois RE. The natural history of untreated asymptomatic osteonecrosis of the femoral head: a systematic literature review. *J Bone Joint Surg Am* 2010; **92**: 2165-2170 [*RCA*] [PMID: 20844158 DOI: 10.2106/JBJS.I.00575] [Full Text]
7 **Fukushima W**, Fujioka M, Kubo T, Tamakoshi A, Nagai M, Hirota Y. Nationwide epidemiologic survey of idiopathic osteonecrosis of the femoral head. *Clin Orthop Relat Res* 2010; **468**: 2715-2724 [*RCA*] [PMID: 20224959 DOI: 10.1007/s11999-010-1292-x] [FullText] [Full Text (PDF)]
8 **Powell C**, Chang C, Naguwa SM, Cheema G, Gershwin ME. Steroid induced osteonecrosis: An analysis of steroid dosing risk. *Autoimmun Rev* 2010; **9**: 721-743 [*RCA*] [PMID: 20621176 DOI: 10.1016/j.autrev.2010.06.007] [FullText] [Full Text(PDF)]
9 **Matsuo K**, Hirohata T, Sugioka Y, Ikeda M, Fukuda A. Influence of alcohol intake, cigarette smoking, and occupational status on idiopathic osteonecrosis of the femoral head. *Clin Orthop Relat Res* 1988; 115-123 [*RCA*] [PMID: 3409564] [FullText]
10 **Suh KT**, Kim SW, Roh HL, Youn MS, Jung JS. Decreased osteogenic differentiation of mesenchymal stem cells in alcohol-induced osteonecrosis. *Clin Orthop Relat Res* 2005; 220-225 [*RCA*] [PMID: 15685079 DOI: 10.1097/01.blo.0000150568.16133.3c] [FullText]
11 **Hernigou P**, Habibi A, Bachir D, Galacteros F. The natural history of asymptomatic osteonecrosis of the femoral head in adults with sickle cell disease. *J Bone Joint Surg Am* 2006; **88**: 2565-2572 [*RCA*] [PMID: 17142405 DOI: 10.2106/JBJS.E.01455] [FullText]
12 **Kaushik AP**, Das A, Cui Q. Osteonecrosis of the femoral head: An update in year 2012. *World J Orthop* 2012; **3**: 49-57 [*RCA*] [PMID: 22655222 DOI: 10.5312/wjo.v3.i5.49] [FullText] [Full Text(PDF)]
13 **Pittenger MF**, Discher DE, Péault BM, Phinney DG, Hare JM, Caplan AI. Mesenchymal stem cell perspective: cell biology to clinical progress. *NPJ Regen Med* 2019; **4**: 22 [*RCA*] [PMID: 31815001 DOI: 10.1038/s41536-019-0083-6] [FullText] [Full Text(PDF)]
14 **Gangji V**, Hauzeur JP. Treatment of osteonecrosis of the femoral head with implantation of autologous bone-marrow cells. Surgical technique. *J Bone Joint Surg Am* 2005; **87** Suppl 1: 106-112 [*RCA*] [PMID: 15743852 DOI: 10.2106/JBJS.D.02662] [FullText]
15 **Hernigou P**, Beaujean F, Lambotte JC. Decrease in the mesenchymal stem-cell pool in the proximal femur in corticosteroid-induced osteonecrosis. *J Bone Joint Surg Br* 1999; **81**: 349-355 [*RCA*] [PMID: 10204950 DOI: 10.1302/0301-620x.81b2.8818] [FullText]
16 **Wang BL**, Sun W, Shi ZC, Lou JN, Zhang NF, Shi SH, Guo WS, Cheng LM, Ye LY, Zhang WJ, Li ZR. Decreased proliferation of mesenchymal stem cells in corticosteroid-induced osteonecrosis of femoral head. *Orthopedics* 2008; **31**: 444 [*RCA*] [PMID: 19292322 DOI: 10.3928/01477447-20080501-33] [FullText]
17 **Wang M**, Liao Q, Zhou B, Qiu ZQ, Cheng LM. [Preliminary study of influence of bone tissue from osteonecrosis of femoral head on the proliferation and differentiation of canine bone marrow mesenchymal stem cells]. *Zhonghua Yi Xue Za Zhi* 2013; **93**: 856-859 [*RCA*] [PMID: 23859395] [FullText]
18 **Mont MA**, Hungerford DS. Non-traumatic avascular necrosis of the femoral head. *J Bone Joint Surg Am* 1995; **77**: 459-474 [*RCA*] [PMID: 7890797 DOI: 10.2106/00004623-199503000-00018] [FullText]

19 **Novack DV**. Role of NF-κB in the skeleton. *Cell Res* 2011; **21**: 169-182 [*RCA*] [PMID: 21079651 DOI: 10.1038/cr.2010.159] [FullText]

20 **Liu-Bryan R**, Terkeltaub R. Emerging regulators of the inflammatory process in osteoarthritis. *Nat Rev Rheumatol* 2015; **11**: 35-44 [*RCA*] [PMID: 25266449 DOI: 10.1038/nrrheum.2014.162] [FullText]

21 **Cardín-Pereda A**, García-Sánchez D, Terán-Villagrá N, Alfonso-Fernández A, Fakkas M, Pérez-Del Barrio A, Marín-Díez E, Fernández-Lobo V, Sanz-Bellón P, Montes-Figueroa E, Lamprecht Y, Pérez-Campo FM. Diagnostic Reliability of Plain Radiography in Osteonecrosis of the Femoral Head: General Radiological Features Revised. *Curr Med Imaging* 2023 [*RCA*] [PMID: 37649291 DOI: 10.2174/1573405620666230829150229] [FullText]

22 **Del Real A**, Pérez-Campo FM, Fernández AF, Sañudo C, Ibarbia CG, Pérez-Núñez MI, Criekinge WV, Braspenning M, Alonso MA, Fraga MF, Riancho JA. Differential analysis of genome-wide methylation and gene expression in mesenchymal stem cells of patients with fractures and osteoarthritis. *Epigenetics* 2017; **12**: 113-122 [*RCA*] [PMID: 27982725 DOI: 10.1080/15592294.2016.1271854] [FullText]

23 **García-Sánchez D**, González-González A, García-García P, Reyes R, Pérez-Núñez MI, Riancho JA, Évora C, Rodríguez-Rey JC, Pérez-Campo FM. Effective Osteogenic Priming of Mesenchymal Stem Cells through LNA-ASOs-Mediated Sfrp1 Gene Silencing. *Pharmaceutics* 2021; **13**: 1277 [*RCA*] [PMID: 34452242 DOI: 10.3390/pharmaceutics13081277] [FullText] [Full Text(PDF)]

24 **Gregory CA**, Gunn WG, Peister A, Prockop DJ. An Alizarin red-based assay of mineralization by adherent cells in culture: comparison with cetylpyridinium chloride extraction. *Anal Biochem* 2004; **329**: 77-84 [*RCA*] [PMID: 15136169 DOI: 10.1016/j.ab.2004.02.002] [FullText]

25 **Kraus NA**, Ehebauer F, Zapp B, Rudolphi B, Kraus BJ, Kraus D. Quantitative assessment of adipocyte differentiation in cell culture. *Adipocyte* 2016; **5**: 351-358 [*RCA*] [PMID: 27994948 DOI: 10.1080/21623945.2016.1240137] [FullText]

26 **Delgado-Calle J**, Sañudo C, Sánchez-Verde L, García-Renedo RJ, Arozamena J, Riancho JA. Epigenetic regulation of alkaline phosphatase in human cells of the osteoblastic lineage. *Bone* 2011; **49**: 830-838 [*RCA*] [PMID: 21700004 DOI: 10.1016/j.bone.2011.06.006] [FullText]

27 **Collart MA**, Baeuerle P, Vassalli P. Regulation of tumor necrosis factor alpha transcription in macrophages: involvement of four kappa B-like motifs and of constitutive and inducible forms of NF-kappa B. *Mol Cell Biol* 1990; **10**: 1498-1506 [*RCA*] [PMID: 2181276 DOI: 10.1128/mcb.10.4.1498-1506.1990] [FullText]

28 **Hayden MS**, Ghosh S. NF-κB, the first quarter-century: remarkable progress and outstanding questions. *Genes Dev* 2012; **26**: 203-234 [*RCA*] [PMID: 22302935 DOI: 10.1101/gad.183434.111] [FullText]

29 **Tanaka T**, Narazaki M, Kishimoto T. IL-6 in inflammation, immunity, and disease. *Cold Spring Harb Perspect Biol* 2014; **6**: a016295 [*RCA*] [PMID: 25190079 DOI: 10.1101/cshperspect.a016295] [FullText]

30 **Houdek MT**, Wyles CC, Packard BD, Terzic A, Behfar A, Sierra RJ. Decreased Osteogenic Activity of Mesenchymal Stem Cells in Patients With Corticosteroid-Induced Osteonecrosis of the Femoral Head. *J Arthroplasty* 2016; **31**: 893-898 [*RCA*] [PMID: 26404846 DOI: 10.1016/j.arth.2015.08.017] [FullText]

31 **Wu ZY**, Sun Q, Liu M, Grottkau BE, He ZX, Zou Q, Ye C. Correlation between the efficacy of stem cell therapy for osteonecrosis of the femoral head and cell viability. *BMC Musculoskelet Disord* 2020; **21**: 55 [*RCA*] [PMID: 31996187 DOI: 10.1186/s12891-020-3064-4] [Full Text] [Full Text(PDF)]

32 **Sultan NA**, Hamama HH, Grawish ME, El-Toukhy RI, Mahmoud SH. Impact of different capping materials extracts on proliferation and osteogenic differentiation of cultured human dental pulp stem cells. *Sci Rep* 2025; **15**: 11140 [*RCA*] [PMID: 40169700 DOI: 10.1038/s41598-025-93759-y] [FullText] [Full Text(PDF)]

33 **Tabera S**, Pérez-Simón JA, Díez-Campelo M, Sánchez-Abarca LI, Blanco B, López A, Benito A, Ocio E, Sánchez-Guijo FM, Cañizo C, San Miguel JF. The effect of mesenchymal stem cells on the viability, proliferation and differentiation of B-lymphocytes. *Haematologica* 2008; **93**: 1301-1309 [*RCA*] [PMID: 18641017 DOI: 10.3324/haematol.12857] [FullText]

34 **Wang JJ**, Liu YL, Sun YC, Ge W, Wang YY, Dyce PW, Hou R, Shen W. Basic Fibroblast Growth Factor Stimulates the Proliferation of Bone Marrow Mesenchymal Stem Cells in Giant Panda (Ailuropoda melanoleuca). *PLoS One* 2015; **10**: e0137712 [*RCA*] [PMID: 26375397 DOI: 10.1371/journal.pone.0137712] [FullText] [Full Text(PDF)]

35 **Hayden MS**, West AP, Ghosh S. NF-kappaB and the immune response. *Oncogene* 2006; **25**: 6758-6780 [*RCA*] [PMID: 17072327 DOI: 10.1038/sj.onc.1209943] [FullText]

36 **Rosen CJ**, Ackert-Bicknell C, Rodriguez JP, Pino AM. Marrow fat and the bone microenvironment: developmental, functional, and pathological implications. *Crit Rev Eukaryot Gene Expr* 2009; **19**: 109-124 [*RCA*] [PMID: 19392647 DOI: 10.1615/critreveukargeneexpr.v19.i2.20] [FullText] [Full Text(PDF)]

37 **Walewska A**, Janucik A, Tynecka M, Moniuszko M, Eljaszewicz A. Mesenchymal stem cells under epigenetic control - the role of epigenetic machinery in fate decision and functional properties. *Cell Death Dis* 2023; **14**: 720 [*RCA*] [PMID: 37932257 DOI: 10.1038/s41419-023-06239-4] [FullText]

38 **Devlin MJ**, Rosen CJ. The bone-fat interface: basic and clinical implications of marrow adiposity. *Lancet Diabetes Endocrinol* 2015; **3**: 141-147 [*RCA*] [PMID: 24731667 DOI: 10.1016/S2213-8587(14)70007-5] [FullText]

39 **Whyte MP**. Physiological role of alkaline phosphatase explored in hypophosphatasia. *Ann N Y Acad Sci* 2010; **1192**: 190-200 [*RCA*] [PMID: 20392236 DOI: 10.1111/j.1749-6632.2010.05387.x] [FullText]

40 **Adamopoulos IE**. Inflammation in bone physiology and pathology. *Curr Opin Rheumatol* 2018; **30**: 59-64 [*RCA*] [PMID: 29016371 DOI: 10.1097/BOR.0000000000000449] [FullText]

41 **Chang J**, Liu F, Lee M, Wu B, Ting K, Zara JN, Soo C, Al Hezaimi K, Zou W, Chen X, Mooney DJ, Wang CY. NF-κB inhibits osteogenic differentiation of mesenchymal stem cells by promoting β-catenin degradation. *Proc Natl Acad Sci U S A* 2013; **110**: 9469-9474 [*RCA*] [PMID: 23690607 DOI: 10.1073/pnas.1300532110] [FullText]

42 **Waterman RS**, Tomchuck SL, Henkle SL, Betancourt AM. A new mesenchymal stem cell (MSC) paradigm: polarization into a pro-inflammatory MSC1 or an Immunosuppressive MSC2 phenotype. *PLoS One* 2010; **5**: e10088 [*RCA*] [PMID: 20436665 DOI: 10.1371/journal.pone.0010088] [FullText] [Full Text(PDF)]

43 **Chen F**, Gu M, Xu H, Zhou S, Shen Z, Li X, Dong L, Li P. Chronic intermittent hypoxia impairs BM-MSC osteogenesis and long bone growth through regulating histone lactylation. *J Transl Med* 2025; **23**: 845 [*RCA*] [PMID: 40722170 DOI: 10.1186/s12967-025-06849-w] [FullText] [Full Text(PDF)]

44 **Ding M**, Cheng Y, Xu Z, Lu Y, Li J, Lu L, Zong M, Fan L. Hypoxia Inhibits Osteogenesis and Promotes Adipogenesis of Fibroblast-like Synoviocytes *via* Upregulation of Leptin in Patients with Rheumatoid Arthritis. *J Immunol Res* 2022; **2022**: 1431399 [*RCA*] [PMID: 36530571 DOI: 10.1155/2022/1431399] [FullText]

45 **Justesen J**, Stenderup K, Ebbesen EN, Mosekilde L, Steiniche T, Kassem M. Adipocyte tissue volume in bone marrow is increased with aging

and in patients with osteoporosis. *Biogerontology* 2001; **2**: 165-171 [*RCA*] [PMID: 11708718 DOI: 10.1023/a:1011513223894] [FullText]

46 **García-García P**, Reyes R, García-Sánchez D, Pérez-Campo FM, Rodríguez-Rey JC, Évora C, Díaz-Rodríguez P, Delgado A. Nanoparticle-mediated selective Sfrp-1 silencing enhances bone density in osteoporotic mice. *J Nanobiotechnology* 2022; **20**: 462 [*RCA*] [PMID: 36309688 DOI: 10.1186/s12951-022-01674-5] [FullText] [Full Text(PDF)]

47 **Tang H**, Ling T, Zhao E, You M, Chen X, Chen G, Zhou K, Zhou Z. The efficacy of core decompression combined with regenerative therapy in early femoral head necrosis: a systematic review and meta-analysis involving 954 subjects. *Front Pharmacol* 2024; **15**: 1501590 [*RCA*] [PMID: 39840080 DOI: 10.3389/fphar.2024.1501590] [FullText]

48 **Hernigou P**, Homma Y, Hernigou J, Flouzat Lachaniette CH, Rouard H, Verrier S. Mesenchymal Stem Cell Therapy for Bone Repair of Human Hip Osteonecrosis with Bilateral Match-Control Evaluation: Impact of Tissue Source, Cell Count, Disease Stage, and Volume Size on 908 Hips. *Cells* 2024; **13**: 776 [*RCA*] [PMID: 38727312 DOI: 10.3390/cells13090776] [FullText]

49 **Daltro GC**, Fortuna V, de Souza ES, Salles MM, Carreira AC, Meyer R, Freire SM, Borojevic R. Efficacy of autologous stem cell-based therapy for osteonecrosis of the femoral head in sickle cell disease: a five-year follow-up study. *Stem Cell Res Ther* 2015; **6**: 110 [*RCA*] [PMID: 26021713 DOI: 10.1186/s13287-015-0105-2] [FullText] [Full Text(PDF)]

Published by **Baishideng Publishing Group Inc**
7041 Koll Center Parkway, Suite 160, Pleasanton, CA 94566, USA
**Telephone:** +1-925-3991568
**E-mail:** office@baishideng.com
**Help Desk:** https://www.f6publishing.com/helpdesk
https://www.wjgnet.com